

Reaction path optimization and vibrational frequency analysis via *ab initio* QM/MM free energy gradient (FEG) method: application to isomerization process of glycine in aqueous solution

Norio Takenaka · Yukichi Kitamura ·
Yoshiyuki Koyano · Toshio Asada ·
Masataka Nagaoka

Received: 21 February 2011 / Accepted: 13 May 2011 / Published online: 31 May 2011
© Springer-Verlag 2011

Abstract For the purpose to explore reaction paths accurately for chemical reaction systems in solution, we have proposed the free energy gradient (FEG) method combined with *ab initio* QM/MM–MD calculation, i.e., the *ab initio* QM/MM–FEG method. For demonstration, the method has been applied to the isomerization reaction of glycine in aqueous solution, i.e., the intramolecular proton transfer reaction from zwitterion (ZW) to the neutral form (NF). Including the solvent effect explicitly by the *ab initio* QM/MM–FEG method, those stable-state structures were found different from those obtained in gas phase and by an implicit dielectric continuum model at the same *ab initio* QM level. Additionally, by the vibration frequency analysis with the “free energy (FE)” hessian in solution, the calculated vibrational frequencies were in good agreement with the experimental ones in the range from low to middle frequency of ZW. Furthermore, the FE of activation from ZW to NF was found in very good agreement with not only the estimation by the Car-Parrinello MD method but also by the previous experimental one. It is concluded that the *ab initio* QM/MM–FEG method is promising and should

provide a better description of chemical reaction systems in solution in comparison with a number of conventional approaches by using the mean field approximations.

Keywords Free energy gradient (FEG) method · *Ab initio* QM/MM–FEG method · Chemical reaction systems in solution · Intramolecular proton transfer · Glycine · Free energy (FE) hessian · FEG–NEB method · Free energy of activation · Vibrational frequency analysis

1 Introduction

The atomistic computer simulation methods can provide us with microscopic information such as the transition state (TS) structure that is not able to be observed easily by conventional experimental approaches. So far, quantum mechanical (QM) approaches using semiempirical and *ab initio* molecular orbital (MO) methods have been carried out for many reaction systems in solutions and biological environment [1–8]. However, for the solution chemical reaction system, it is still difficult to obtain TS geometries because such reactions are involved in both solute species and a vast number of solvent molecules. The potential energy surfaces (PESs) for the solution reaction system are too high dimensional, and then it is almost impossible to search even a TS with respect to all degrees of freedom for the whole system. In such cases, the free energy surface (FES) has been often estimated approximately along only a certain reaction coordinate since FES makes it possible to consider effectively a vast number of solvent molecules. However, the stable-state (SS) and TS geometries should be optimized with respect to all degrees of freedom of the solute in solution for the purpose to indentify these accurate structures on the FES.

Dedicated to Professor Shigeru Nagase on the occasion of his 65th birthday and published as part of the Nagase Festschrift Issue.

N. Takenaka · Y. Kitamura · Y. Koyano · M. Nagaoka (✉)
Graduate School of Information Science, Nagoya University,
Furo-cho, Chikusa-ku, Nagoya 464-8601, Japan
e-mail: mnagaoka@is.nagoya-u.ac.jp
URL: <http://www.ncube.human.nagoya-u.ac.jp/>

T. Asada
Graduate School of Science, Osaka Prefecture University,
1-1 Gakuen-cho, Naka-ku, Sakai, Osaka 599-8531, Japan

N. Takenaka · Y. Koyano · T. Asada · M. Nagaoka
JST-CREST, Kawaguchi 330-0012, Japan

Until now, in solution chemistry, a number of theoretical methods have been developed to identify the SS and TS geometries, taking the solvent effects into consideration [5, 9]. Among them, the dielectric continuum models (DCMs) are such methods that replace the solvent molecules around the solute by a dielectric continuum [5]. The DCMs are often used in the cases of requiring highly accurate QM calculation with relatively low calculation cost. However, they have some problems such as the incorrectness of direct intermolecular interactions of hydrogen bonds (HBs) between solutes and solvent molecules.

On the contrary, the full-atomic molecular dynamics (MD) method can consider legitimately the HB interaction more explicitly as a sum of the interatomic interactions between solutes and solvent molecules for the instantaneous structural arrangements of solvent molecules. As one MD method using the QM calculation, the well-known Car-Parrinello MD (CP-MD) method is with a number of applications for solution chemistry [10]. In the CP-MD method, the motions of both electrons and nuclei are calculated at the same time by introducing the additional equations of motion for the wave function of electrons. However, the direct applications of the CP-MD method are still computationally very expensive and are then restricted to those systems with a small number of atoms. On the other hand, the quantum mechanical/molecular mechanical (QM/MM) method is often utilized as another alternative treatment that only the reactive parts in the whole system are treated quantum mechanically, while the other parts are treated molecular mechanically. The QM/MM method then enables to reduce the computational cost drastically.

Accordingly, the MD method combined with the QM/MM method (QM/MM-MD method) [11] is very useful as a statistical sampling method to treat the whole solution reaction system. The chemical accuracy in QM/MM calculations depends strongly on description of the QM subsystem. Since ab initio QM representations have been shown to provide good chemical accuracy in studies on gas-phase reactions of small molecules, a number of studies on solution reactions have been even executed using ab initio QM/MM-MD calculations. In many of them, further approximate treatments have been introduced to reduce the great computational cost of the QM calculation.

Under the circumstances, being analogous to the energy gradient method on the Born–Oppenheimer (BO) PES in MO theory, we have been developing the free energy gradient (FEG) method [9], utilizing the forces on the FES. In the first application of the FEG method [12–14], we have optimized the molecular geometry of a glycine molecule on the FES in aqueous solution by using the MD method combined with the empirical valence bond (EVB) method [15], i.e., the EVB-FEG method. Then, by using the

QM/MM-MD method and executing both the low-cost semiempirical QM and MM calculation on the fly, the direct “semiempirical QM/MM-FEG method” has been more plausibly applied to identify not only the SS of molecular structures but also their TS in solution [16–22].

Although these methods can explore the FES at the low calculation cost, they require the calibration of a number of empirical parameters for the purpose to apply to the actual system such as the solution reaction system. However, such parameterization is generally time-consuming and it is hard to obtain suitable reference quantities in solution reaction system, e.g., structures and spectroscopic data. Additionally, the calculation results by using these methods cannot be compared with those by the more approximate methods, such as the DCM method, which generally adopt the ab initio MO method for the solute. Therefore, in these simulations, it is difficult to distinguish those errors originating in the parameterization from those by the improvement using the methods.

In this article, for the purpose to further improve the accuracy and applicability of the FEG method, we have, therefore, proposed the FEG method combined directly with the direct ab initio QM/MM-MD method, i.e., the ab initio QM/MM-FEG method, in conjunction with the nudged elastic band (NEB) reaction path optimization method reinforced by the concurrent high-performance computing system. This FEG-NEB method enables us to discuss the differences in the theoretical treatment between the FEG method and other approximate ones at ab initio QM level, in addition to the reaction path in solution. For demonstration, we have applied it to the intramolecular proton transfer reaction of glycine in aqueous solution, i.e., the pathway optimization from zwitterion (ZW) to neutral form (NF). Among a number of solution chemical reactions, the glycine isomerization has been widely studied not only experimentally [23–27] but also theoretically [12–14, 28–42] by several groups for its pivotal biochemical importance. In the present study, we have optimized not only the molecular structures but also the reaction path on the FES, for the first time, by the ab initio QM/MM-FEG method. After introducing briefly the methodology for the QM/MM-MD simulation and the ab initio QM/MM-FEG method in Sect. 2, we present results and discussion in Sect. 3. Finally, the main results are summarized in Sect. 4.

2 Theory and computational methods

2.1 Ab initio QM/MM-MD method

For the glycine aqueous solution, we adopted ab initio QM/MM-MD method for the purpose to make a lot of

configurations of the instantaneous solvent structures reflected explicitly in the solute electronic state. Presently, a solute glycine molecule was taken as a QM part which is described by ab initio MO method at the Hartree–Fock (HF) or the second-order Møller–Plesset (MP2) perturbation theory with 6-31+G(d) basis sets. On the other hand, the MM solvent water molecules were taken as the remaining MM part where each water molecule is represented by the rigid TIP3P model [43].

In the ab initio QM/MM–MD method, the equations of motion of the solute–solvent system were written as follows.

$$m_i \frac{d^2 \mathbf{r}_i}{dt^2} = -\nabla_i \hat{H}, \quad (1)$$

where m_i is the mass of atom i and \mathbf{r}_i is its Cartesian coordinates, in general, and the Hamiltonian \hat{H} consists of three terms:

$$\hat{H} = \hat{H}_{\text{QM}} + \hat{H}_{\text{MM}} + \hat{H}_{\text{QM/MM}}, \quad (2)$$

where the first two terms \hat{H}_{QM} and \hat{H}_{MM} stand for the standard Hamiltonian of the QM and MM systems, respectively, while the last QM/MM term $\hat{H}_{\text{QM/MM}}$ does for the interaction between the QM and MM system, and is expressed as a sum of electrostatic (est) and van der Waals (vdW) terms:

$$\hat{H}_{\text{QM/MM}} = \hat{H}_{\text{QM/MM}}^{\text{est}} + \hat{H}_{\text{QM/MM}}^{\text{vdW}}. \quad (3)$$

The est term $\hat{H}_{\text{QM/MM}}^{\text{est}}$ is given by

$$\hat{H}_{\text{QM/MM}}^{\text{est}} = \sum_M q_M V_{\text{QM}}(\mathbf{R}_M), \quad (4)$$

with the potential

$$V_{\text{QM}}(\mathbf{R}_M) = -\sum_s \frac{1}{R'_{sM}} + \sum_A \frac{Z_A}{R_{AM}}, \quad (5)$$

which is represented as the sum of coulomb interactions created by the electrons and cores of QM atoms. In these expressions, q_M is the atomic point electric charge on the M th MM atom in solvent water molecules, \mathbf{R}_M is its Cartesian coordinates, R'_{sM} is the distance between the s th QM electron of the solute glycine molecule and the M th MM atom, Z_A is the core charge of the A th QM atom, and R_{AM} is the distance between the A th QM atom and the M th MM one. The vdW term $\hat{H}_{\text{QM/MM}}^{\text{vdW}}$ is expressed using a number of 6–12 Lennard–Jones (LJ) functions:

$$\hat{H}_{\text{QM/MM}}^{\text{vdW}} = \sum_A \sum_M \varepsilon_{AM} \left[\left(\frac{r_{AM}}{R_{AM}} \right)^{12} - 2 \left(\frac{r_{AM}}{R_{AM}} \right)^6 \right], \quad (6)$$

where ε_{AM} and r_{AM} are a couple of LJ parameters for the A th QM atom interacting with the M th MM atom. In this

study, the general AMBER force field (GAFF) [44] was used to describe LJ interactions between the solute QM glycine and solvent MM water molecules. The total system potential energy V is then given by

$$V = \langle \psi | \hat{H}_{\text{QM}} + \hat{H}_{\text{QM/MM}} | \psi \rangle + V_{\text{MM}} \quad (7a)$$

$$= V_{\text{SB}} + V_{\text{MM}}. \quad (7b)$$

For the purpose to execute the direct ab initio QM/MM–MD simulation, we used an original version of AMBER–GAUSSIAN interface (AG–IF) [45], by combining the ROAR2.1 module [46] of MD simulation program package AMBER 7.0 [47] with the ab initio MO program GAUSSIAN03 [48].

2.2 Stable-state optimization: Free energy gradient method

We have developed the ab initio QM/MM–FEG method for applications to identify the optimized structures and reaction path for solution reaction system at the ab initio QM level. According to the equilibrium statistical thermodynamics, in an equilibrium system, for example, the canonical (NVT) ensemble average of an observable is to be replaced as the time average calculated over a long enough NVT equilibrium QM/MM–MD trajectory, provided the trajectory is ergodic. Then, the force $\mathbf{F}^{\text{FE}}(\mathbf{q}^{\text{S}})$ on the NVT FES is equal to the time average of the force acting on each atom of the solute molecule with the geometry \mathbf{q}^{S} .

$$\mathbf{F}^{\text{FE}}(\mathbf{q}^{\text{S}}) = -\frac{\partial A(\mathbf{q}^{\text{S}})}{\partial \mathbf{q}^{\text{S}}} = -\left\langle \frac{\partial V_{\text{SB}}(\mathbf{q}^{\text{S}})}{\partial \mathbf{q}^{\text{S}}} \right\rangle, \quad (8)$$

where the Helmholtz free energy $A(\mathbf{q}^{\text{S}})$ is a state function of not only thermodynamic variables (N , V , T) but also the solute structure \mathbf{q}^{S} . In Eq. 8, the brackets denote the equilibrium NVT ensemble average,

$$\langle \dots \rangle = \frac{\int d\mathbf{q}^{\text{B}} (\dots) \exp(-\beta V(\mathbf{q}^{\text{S}}))}{\int d\mathbf{q}^{\text{B}} \exp(-\beta V(\mathbf{q}^{\text{S}}))}, \quad (9)$$

where \mathbf{q}^{B} denotes the solvent coordinates as a whole, β denotes $1/k_{\text{B}}T$, and V is the potential energy of the whole solution system. By the free energy perturbation (FEP) theory [49], the FE difference at an optimization cycle i , ΔA_i , is described as follows:

$$\begin{aligned} \Delta A_i &= A_{i+1} - A_i, \\ &= -k_{\text{B}}T \ln \langle \exp[-\beta \{V_{\text{SB}}(\mathbf{q}_{i+1}^{\text{S}}) - V_{\text{SB}}(\mathbf{q}_i^{\text{S}})\}] \rangle_i \end{aligned} \quad (10)$$

where \mathbf{q}_i^{S} and $\mathbf{q}_{i+1}^{\text{S}}$ are solute structures at the optimization step i and $i+1$, respectively. The subscript i in the average $\langle \dots \rangle_i$ in Eq. 10 means that the average is taken over the sampling at \mathbf{q}_i^{S} :

$$\langle \dots \rangle_i = \frac{\int d\mathbf{q}^B(\dots) \exp(-\beta V_{SB}(\mathbf{q}_{i+1}^s))}{\int d\mathbf{q}^B \exp(-\beta V_{SB}(\mathbf{q}_i^s))}. \quad (11)$$

By applying the L-BFGS algorithm [50], the optimization cycle was repeated for the FEP treatment, until the following condition is satisfied, i.e., the zero gradient condition:

$$\left\langle \frac{\partial V_{SB}(\mathbf{q}^s)}{\partial \mathbf{q}^s} \right\rangle_i \approx 0. \quad (12)$$

2.3 Reaction path optimization: FEG–NEB method

To optimize the TS structure on the FES for the solution reaction system, we prepared the chain-of-conformations $\{\mathbf{q}_{i,l}^s | l = 0, \dots, N\}$, which is an N discrete representation out of the solute structures connecting the reactant state (RS) and product state (PS), which corresponds to those two states at $l = 0$ and $l = N$, respectively. In this study, we employed the NEB method [51], which is one of the reaction path optimization methods to optimize the chain-of-conformations as a whole. In the ab initio QM/MM–FEG method combined with the NEB method, i.e., the ab initio QM/MM–FEG–NEB method, the force on the FES for the l th structure at the optimization step i , $\mathbf{F}_{i,l}^{\text{FE}}(\mathbf{q}_{i,l}^s)$, is calculated in the following way:

$$\mathbf{F}_{i,l}^{\text{FE}}(\mathbf{q}_{i,l}^s) = \mathbf{F}_{i,l}^{\parallel}(\mathbf{q}_{i,l}^s) + \mathbf{F}_{i,l}^{\perp}(\mathbf{q}_{i,l}^s), \quad (13a)$$

$$\mathbf{F}_{i,l}^{\parallel}(\mathbf{q}_{i,l}^s) = \left\{ \left(k \left| \mathbf{q}_{i,l+1}^s - \mathbf{q}_{i,l}^s \right| - k \left| \mathbf{q}_{i,l}^s - \mathbf{q}_{i,l-1}^s \right| \right) \cdot \boldsymbol{\tau}_{i,l} \right\} \boldsymbol{\tau}_{i,l}, \quad (13b)$$

$$\mathbf{F}_{i,l}^{\perp}(\mathbf{q}_{i,l}^s) = -\frac{\partial A(\mathbf{q}_{i,l}^s)}{\partial \mathbf{q}^s} + \left(\frac{\partial A(\mathbf{q}_{i,l}^s)}{\partial \mathbf{q}^s} \cdot \boldsymbol{\tau}_{i,l} \right) \boldsymbol{\tau}_{i,l}, \quad (13c)$$

and

$$\boldsymbol{\tau}_{i,l} = \frac{(\mathbf{q}_{i,l+1}^s - \mathbf{q}_{i,l}^s)}{\left| \mathbf{q}_{i,l+1}^s - \mathbf{q}_{i,l}^s \right|}, \quad (13d)$$

where, $\mathbf{F}_{i,l}^{\parallel}(\mathbf{q}_{i,l}^s)$ denotes the parallel component of $\mathbf{F}_{i,l}^{\text{FE}}(\mathbf{q}_{i,l}^s)$ for the l th configuration at the optimization step i , $\mathbf{F}_{i,l}^{\perp}(\mathbf{q}_{i,l}^s)$ is the perpendicular one and $\boldsymbol{\tau}_{i,l}$ represents the projection vector to the direction of the reaction coordinate. Additionally, we employed 300 kcal/(mol Å²) as the value of the spring constant k . It is until the zero gradient condition (Eq. 12) is satisfied independently for all the N configurations on the chain-of-conformations,

$$\left\{ \mathbf{F}_{i,l}^{\text{FE}}(\mathbf{q}_{i,l}^s) \approx 0 | l = 0, \dots, N \right\}, \quad (14)$$

that the optimization cycles were repeated self-consistently. The FEG–NEB optimization procedure is summarized schematically in Fig. 1.

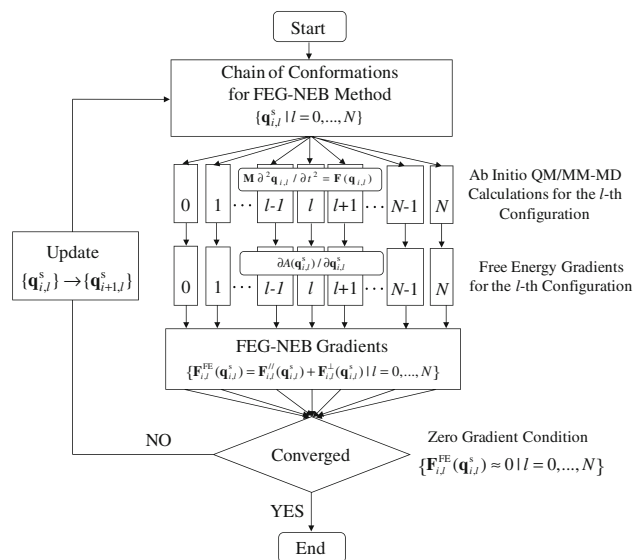


Fig. 1 Reaction path optimization scheme of ab initio QM/MM–FEG–NEB method

2.4 Vibrational frequency analysis: Free energy hessian diagonalization

To certify the SS and TS structure in solution, we performed the vibrational frequency analysis (VFA) by diagonalizing the “free energy (FE)” hessian in solution [9]. In the analysis, we have executed the ab initio QM/MM–MD simulation, calculating directly the elements of the FE hessian matrix, which are described by the following equation [9].

$$\frac{\partial^2 A(\mathbf{q}^s)}{\partial \mathbf{q}^s \partial \mathbf{q}^s} = \left\langle \frac{\partial^2 V_{SB}(\mathbf{q}^s)}{\partial \mathbf{q}^s \partial \mathbf{q}^s} \right\rangle - \frac{1}{k_B T} \left[\left\langle \frac{\partial V_{SB}(\mathbf{q}^s)}{\partial \mathbf{q}^s} \frac{\partial V_{SB}(\mathbf{q}^s)^T}{\partial \mathbf{q}^s} \right\rangle - \left\langle \frac{\partial V_{SB}(\mathbf{q}^s)}{\partial \mathbf{q}^s} \right\rangle \left\langle \frac{\partial V_{SB}(\mathbf{q}^s)}{\partial \mathbf{q}^s} \right\rangle^T \right], \quad (15a)$$

where the superscript T denotes the transposition. In this study, to reduce the simulation time, the FE hessian matrix elements were calculated by using the following approximation,

$$\frac{\partial^2 A(\mathbf{q}^s)}{\partial \mathbf{q}^s \partial \mathbf{q}^s} \simeq \left\langle \frac{\partial^2 V_{SB}(\mathbf{q}^s)}{\partial \mathbf{q}^s \partial \mathbf{q}^s} \right\rangle, \quad (15b)$$

since the contribution of the second term in Eq. 15a was small enough in comparison with that of the first term [21, 52]. Then, we diagonalized the mass-weighted FE hessian matrix,

$$\frac{\partial^2 A(\mathbf{q}^s)}{\partial \sqrt{\mathbf{m}^s} \partial \sqrt{\mathbf{m}^s}} \simeq \frac{1}{\mathbf{m}^s} \left\langle \frac{\partial^2 V_{SB}(\mathbf{q}^s)}{\partial \mathbf{q}^s \partial \mathbf{q}^s} \right\rangle, \quad (15c)$$

where \mathbf{m}^s is the atomic mass matrix of the solute molecule, and obtained the effective normal vibrational frequencies of the solute molecule in solution.

Also in the FEG method, it is a common matter of course that free energetic contribution δA from the degrees of freedom (DOF) for the intramolecular motion of the solute as well as due to the quantum effect is taken into consideration, similarly as the traditional treatment in gas phase [53, 54]. However, in solution, it is interesting to note that those DOFs of such cooperative motions as the whole molecular rotation, etc., correctly defined in gas phase, should turn to be a number of librational motions, some kinds of vibrational ones, and might be dealt with according to the normal vibrational treatment [55]. Therefore, we can approximately estimate also these contributions to δA at the l th reaction coordinate s_l by using a set of effective normal vibrational frequencies $\{v_{l,k}|k = 1, \dots, 3N\}$ of the l th solute structure \mathbf{q}_l^s . These contributions to the FE, δA_l , are defined as follows:

$$A(s_l) = A_l + \delta A_l = A_l + (\delta A_l^{\text{ZPE}} + \delta A_l^{\text{HA}}) \quad (16a)$$

where δA_l^{ZPE} is the contribution of the zero-point energy (ZPE) correction at the l th solute structure,

$$\delta A_l^{\text{ZPE}} = \sum_{k=1}^{3N} \frac{1}{2} h v_{l,k}, \quad (16b)$$

while δA_l^{HA} is that within the harmonic approximation (HA) [53, 54],

$$\delta A_l^{\text{HA}} = k_B T \sum_{k=1}^{3N} \ln \{1 - \exp(-h v_{l,k}/k_B T)\}. \quad (16c)$$

2.5 Computational details

Using a version of AG-IF [45], combining the ROAR2.1 module [46] of MD simulation program package AMBER 7.0 [47] with the ab initio MO program GAUSSIAN03 [48], a number of ab initio QM/MM-MD simulations were performed for a system consisting of a single QM glycine molecule and 515 MM water molecules in a rectangular simulation cell with linear dimensions $L_x = 24.75$, $L_y = 26.12$ and $L_z = 24.14$ Å, which were adjusted initially by executing the classical MD simulation with *NPT* ensemble at 1 atm. In the classical MD simulation, for the effective atomic charges of the solute glycine molecule, we employed the ESP atomic charges obtained by Merz-Kollman scheme [56, 57] at the MP2/6-31+G(d) level of theory. The three-dimensional periodic boundary condition was imposed. The temperature was controlled to 300 K by the Berendsen algorithm so that the system might be maintained to be an *NVT* ensemble. The non-bonded cutoff distance was chosen as 12.0 Å. The velocity Verlet

integrator was used to integrate a set of simultaneous equations of motion, with a time step of 1 fs. After equilibration, the sampling run was executed for 3,000 steps (3 ps) at each FEG optimization cycle and was used to calculate physical quantities by averaging over this equilibrium sampling. All these calculations were done each on 8 cores of Xeon E5345 2.33 GHz QuadCore \times 2.

In such computing systems, the calculation times by using the ab initio QM/MM-FEG method are approximately 1 month until the optimization procedures have been completed (Eq. 12). Since those by using the CPCM method [58], which is one of the DCMs, is approximately 1 h, the present ab initio QM/MM-FEG method was very expensive in comparison with the approximate methods such as the CPCM method. However, the calculation cost of the ab initio QM/MM-FEG method is reduced efficiently by the concurrent computation of the ab initio QM/MM-MD samplings since these equilibrium samplings are independent (Fig. 1), namely the present methods are quite excellent with the parallel computing systems that are rapidly advancing in recent years.

3 Results and discussion

3.1 Glycine in aqueous solution: structures and spectroscopies

According to the ab initio MO electronic structure investigation [28–30], there are various conformers for both ZW and NF. Among them, in the present study, we have focused on a cis-structure, which is often considered to correspond to RS and PS for the intramolecular proton transfer reaction of the glycine molecule in aqueous solution. Therefore, the present ZW and NF are described hereafter as ZW-cis and NF-cis, for convenience.

For the purpose to obtain these SS structures of both ZW-cis and NF-cis, we have estimated molecular geometries of the solute glycine by the ab initio QM/MM-FEG method at the HF/6-31+G(d) and MP2/6-31+G(d) level of theory. Hereafter, we adopt the following abbreviation: the FE calculation by ab initio QM/MM-FEG method, for example, at the HF/6-31+G(d) level, is denoted as FE:HF/6-31+G(d). Then, the FE optimization with respect to all the structural parameters of a glycine molecule, for example, at the HF/6-31+G(d) level, is described by FE:HF/6-31+G(d)//FE:HF/6-31+G(d), and further, the FE calculation at the MP2/6-31+G(d) level for the FE-optimized structure at the HF/6-31+G(d) level is similar by FE:MP2/6-31+G(d)//FE:HF/6-31+G(d). As shown in the first 4 columns next to the mode column in Table 1, we have confirmed, by the VFA in aqueous solution, that any of these four structures obtained by the FEG method has no

Table 1 Normal vibrational frequencies (in cm^{-1}) of the stable state of ZW-cis, NF-cis, and TS of the glycine molecule by the FEG method at the HF/6-31+G(d) and MP2/6-31+G(d) level of theory in aqueous solution, i.e., at the FE:HF/6-31+G(d)//FE:HF/6-31+G(d) and FE:MP2/6-31+G(d)//FE:MP2/6-31+G(d) level

Mode	v (FE:HF/6-31+G(d)//FE:HF/6-31+G(d))		v (FE:MP2/6-31+G(d)//FE:MP2/6-31+G(d))		v (FE:HF/6-31+G(d)//FE:HF/6-31+G(d))
	ZW	NF	ZW	NF	TS
1	71	92	111	34	1,380 <i>i</i>
2	116	98	121	79	91
3	136	116	137	82	109
4	152	120	154	96	127
5	157	131	163	103	136
6	179	155	190	129	153
7	210	166	205	151	179
8	237	353	268	292	241
9	388	388	387	343	520
10	554	580	533	524	543
11	646	618	591	530	639
12	758	717	707	662	755
13	972	944	918	862	848
14	1,036	965	974	866	1,000
15	1,062	1,020	1,077	941	1,026
16	1,220	1,075	1,150	968	1,034
17	1,233	1,186	1,162	1,120	1,260
18	1,442	1,319	1,348	1,206	1,309
19	1,489	1,400	1,372	1,256	1,424
20	1,580	1,484	1,451	1,375	1,479
21	1,624	1,519	1,530	1,389	1,527
22	1,679	1,602	1,557	1,430	1,616
23	1,799	1,611	1,700	1,511	1,677
24	1,844	1,848	1,724	1,722	1,801
25	1,871	1,964	1,728	1,906	1,955
26	3,297	3,267	3,198	3,158	2,184
27	3,361	3,330	3,219	3,219	3,283
28	3,533	3,713	3,278	3,467	3,355
29	3,653	3,740	3,459	3,604	3,683
30	3,700	3,835	3,530	3,698	3,752

imaginary vibrational frequency, showing that they are all true SS structures.

In Fig. 2 shown are the optimized structures of NF-cis in gas phase and those in aqueous solution by the CPCM method at the HF/6-31+G(d) and MP2/6-31+G(d) level of theory, respectively. At the both levels, these structures took the non-planar ones for the C_s symmetric plane of the glycine molecule, c.f., these dihedral angles $\theta(\text{C1-N4-O9-C7})$ range from $\pm 5.4^\circ$ to $\pm 15.6^\circ$. The sign \pm shows two θ s of the two enantiomeric SS structures with respect to C_s symmetric plane of the solute glycine molecule. Additionally, including the electron correlation effect of the electronic state (ES) calculation, the N4-H10 bond lengths, C7-O9-H10 bond angles, and the dihedral angles $\theta(\text{C1-N4-O9-C7})$ of the solute glycine molecule at the MP2 level were found to decrease in comparison with those at the HF

level. The structural differences could be attributed to the stronger intramolecular interactions between N4 and H10 atoms in the solute glycine molecule at the MP2 level.

To explain the geometry differences between the CPCM and FEG method in detail, we have shown, in Fig. 3, the C_s symmetric structures of NF-cis glycine molecule in gas phase ((a) and (d)) and those by the CPCM method ((b) and (e)), which correspond to the TS ones between the “two” non-planar SS ones (i.e., Fig. 2a–d), in addition to those by the FEG method ((c) and (f)) at the HF/6-31+G(d) and MP2/6-31+G(d) level of theory, respectively. In the CPCM method, the NF-cis glycine molecule was found to form the double-well FES with respect to the C_s symmetric plane, as well as the PES in gas phase, whereas the FE difference between these TS and SS structures was very small, e.g., 0.0558–0.176 kcal/mol. On the other hand, it

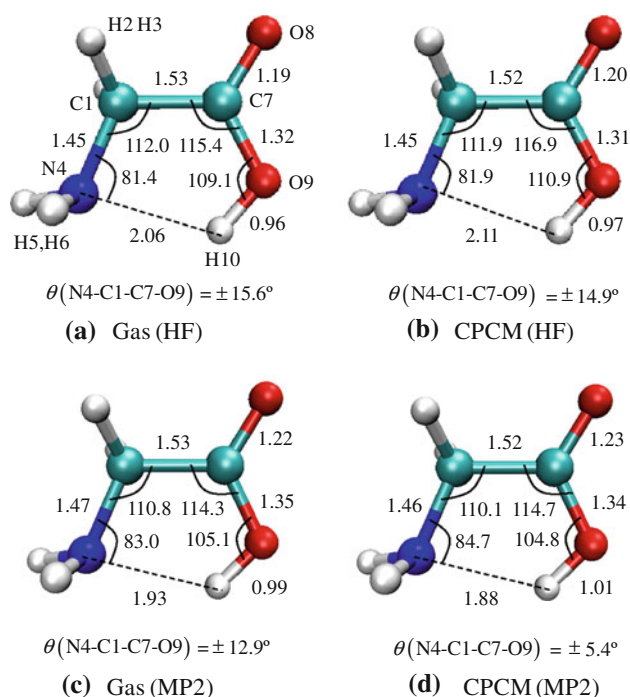
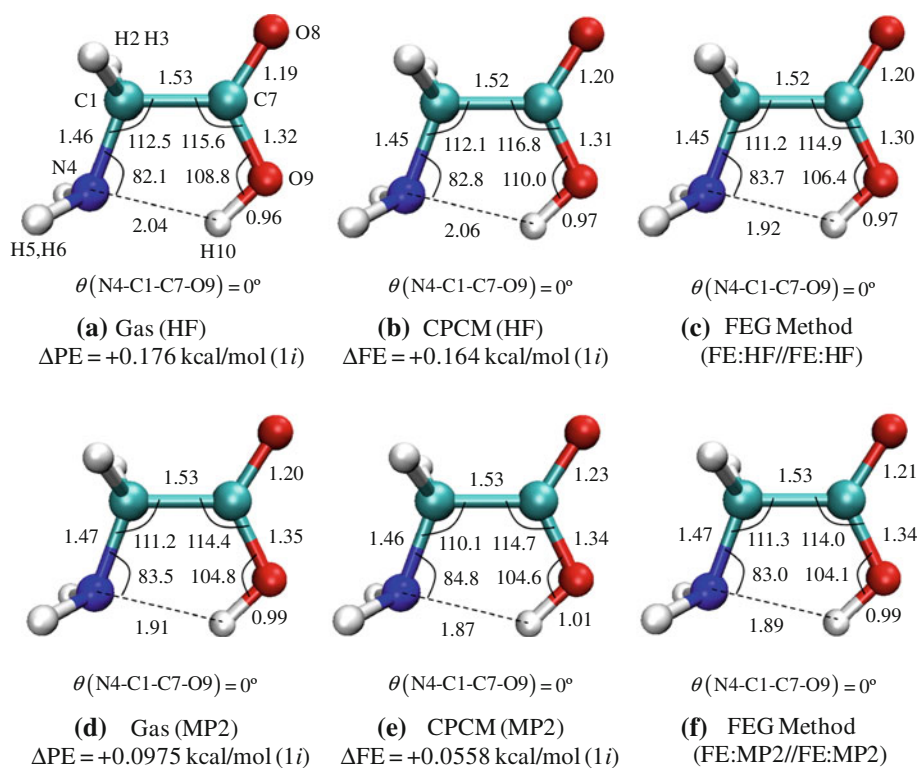


Fig. 2 NF-cis non-planar structures of glycine molecule in gas phase and those in aqueous solution obtained by the CPCM method at the HF/6-31+G(d) and MP2/6-31+G(d) level of theory. Bond lengths are in Å and bond angles are in degree. The sign \pm shows two θ s of the two enantiomeric SS structures with respect to C_s symmetric plane of the solute glycine molecule

Fig. 3 NF-cis planar structures of glycine molecule in gas phase and those in aqueous solution obtained by the CPCM method and the FEG method at the HF/6-31+G(d) and MP2/6-31+G(d) level of theory, respectively. Bond lengths are in Å and bond angles are in degree. Here, **a**, **b**, **d**, and **e** correspond to the transition-state (TS) structures between stable-state (SS) ones shown in Fig. 2, and ΔPE and ΔFE are the difference between their TS and SS ones, respectively



was found that the SS structure by the present FEG method shows a unique planar one, and therefore, the FES takes a single well, not a double well, with respect to the C_s symmetric plane. This can be explained by the reason that such a tiny amount of FE difference as in the CPCM method was smoothed molecular dynamically under the thermodynamic environment (300 K) in aqueous solution. It is said, therefore, that the FEG method should provide a more suitable description of the SS structures in aqueous solution in comparison with the CPCM method.

In Fig. 4 shown are the optimized structures of ZW-cis by the FEG method at the HF/6-31+G(d) and MP2/6-31+G(d) level of theory, respectively. In the CPCM method, there was no SS structure of ZW-cis. Although some methods in the DCMs can provide the SS ones [14, 34, 38], all these structures were reported planar ones, which were unstable in the CPCM method. On the other hand, in the FEG method, the unique non-planar SS structure of ZW-cis was obtained for the first time (Fig. 4). In ZW-cis, the solute glycine molecule forms such a HB network with several ambient solvent waters as in Fig. 5. Due to a few solvent water molecules surrounding the solute glycine molecule, the original C_s symmetry of ZW-cis is broken since those water molecules form a cyclic bridge of HBs between the $-\text{NH}_3$ and $-\text{COO}$ groups, as reported by previous theoretical studies [32, 33, 35–38]. It

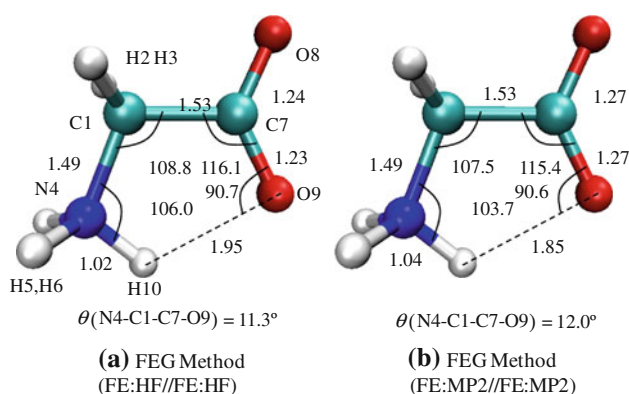


Fig. 4 ZW-cis structures of the glycine molecule in aqueous solution obtained by the FEG method at the HF/6-31+G(d) and MP2/6-31+G(d) level of theory. Bond lengths are in Å and bond angles are in degree

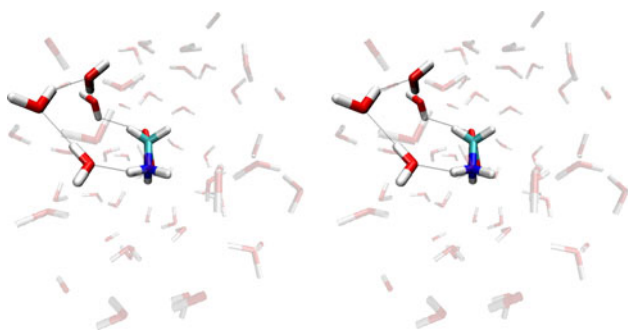


Fig. 5 A typical MD snapshot of the solute ZW-cis glycine molecule in water and the solvent water hydrogen bond network with the $-\text{NH}_3$ and $-\text{COO}$ groups (stereo view)

is interesting that the present HB network, kept quite stable during the MD simulation, corresponds to the most stable SS structures by the cluster model with the 5–7 water molecules [32]. As a result, it is reasonable that the present SS structure of solute glycine molecule was obtained as a non-planar one since the solvent water molecules are pulling $-\text{NH}_3$ and $-\text{COO}$ group to form the HB network. If a solute molecule might have the strong ionic character such as ZW, the explicit treatment of solvent water molecules must be inevitable to obtain the correct SS structures in aqueous solution. In such cases, the FEG method can provide the SS structure that explicitly reflects the contribution of microscopic HBs among solute and solvents.

The vibrational frequencies at the optimized structure of ZW-cis by the FEG method at the MP2 level, scaled by the recommended factor of 0.9486 [59], were compared very well with the experimental Raman frequencies [26] and infrared (IR) ones [27] of glycine in aqueous solution (Table 2). The calculated vibrational frequencies by Eq. 15b were found to increase relatively in comparison with those in gas phase, which were obtained in the condition that only the solvent water molecules might be

removed from this solution system, keeping the glycine structure unchanged. This is attributed to the cage effect of the solvent water molecules around the solute glycine molecule. For example, since the 9th mode corresponds to the bending motion relating to the skeleton C–C–N of the whole glycine, its vibrational frequency must be more sensitive to the cage effect and, therefore, shows larger blue shift than those of other modes.

In particular, it was found that the experimental vibrational frequencies are in good agreement with the present calculated ones at both the low and middle frequency range, which correspond to the vibrational motions of the heavy atoms of glycine molecule. On the other hand, those of the high-frequency modes, which correspond to the C–H and N–H stretching motions of the glycine molecule, were overestimated in comparison with the experimental ones. However, according to the experimental measurements [26, 27], since the high-frequency region of the spectra is broad in its own right, the correct assignment of these vibrational frequencies might be difficult. In addition, there should be the problem that we employed the rigid TIP3P model for solvent water molecules to reduce the computational time. Then, in the present treatment, the O–H stretching motions of the solvent water molecules should not appear and the frequency shifts in the high-frequency region could be restrictive. Using the flexible solvent water model [60, 61], the present-obtained spectra must be more improved.

3.2 Transition state for intramolecular proton transfer reaction of glycine in aqueous solution



For the purpose to obtain the TS structure for the intramolecular proton transfer reaction from ZW-cis to NF-cis of glycine molecule in aqueous solution, we have optimized the chain-of-conformations connecting two SS structures at the RS and PS obtained by ab initio QM/MM–FEG method. First, we prepared a chain-of-conformations that is composed of 10 configurations by the linear interpolation between ZW-cis and NF-cis, and then it was optimized by the ab initio QM/MM–FEG–NEB method at the HF/6-31+G(d) level of theory. As shown in the last column in Table 1, the VFA in aqueous solution has certified actually that the optimized TS structure has only one imaginary frequency. Next, two FE profiles are shown in Fig. 6 for the present intramolecular proton transfer reaction. In the present treatment of the FEG–NEB method, to obtain precise FEs of activation by the FEP method, we further interpolated the successive structures on the chain-of-conformations optimized by the FEG–NEB method. The number of partitions for the FEP treatment was determined so as to obtain the FE differences between the nearest neighbor structures on the interpolated points, which are within 0.6 kcal/mol ($\cong RT(300\text{ K})$). The first FE profile

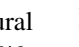
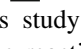
Table 2 Normal vibrational frequencies (in cm^{-1}) scaled by 0.9486^a in aqueous solution and those in gas phase (i.e., only the solvent water molecules are removed from the whole solution system, keeping the glycine structure unchanged) of the stable state of ZW-cis of the

glycine molecule by the FEG method at the MP2/6-31+G(d) level of theory, i.e., at the FE:MP2/6-31+G(d)//FE:MP2/6-31+G(d) level, and the corresponding experimental ones in aqueous solution

Mode	Present		Experiment		Assignments
	Aqueous solution	Gas	Raman ^b	IR ^c	
1	105				
2	115				
3	130				
4	146				
5	155				
6	180				
7	194				
8	254	225			NH ₃ rotating
9	367	257			CCN bending
10	506	471	507	503	CO ₂ rocking
11	561	542	585	608	CO ₂ wagging
12	671	646	671	697	CO ₂ bending
13	871	845	897		CC + CN stretching
14	924	899		893	NH ₂ + CH ₂ twisting
15	1,022	980	1,031		CN + CC stretching
16	1,091	1,031		1,032	NH ₂ twisting
17	1,102	1,047	1,121	1,111	NH ₂ twisting
18	1,279	1,251	1,320	1,332	CH ₂ twisting
19	1,301	1,271	1,330		CH ₂ twisting
20	1,376	1,313	1,412	1,412	CO ₂ symmetric stretching
21	1,451	1,387	1,444	1,510	NH ₃ umbrella + CH ₂ bending
22	1,477	1,452			CH ₂ bending + NH ₃ umbrella
23	1,613	1,600	1,514	1,615	NH ₂ bending
24	1,635	1,618			NH ₂ bending
25	1,639	1,630	1,620		CO ₂ asymmetric stretching
26	3,034	2,990	2,972		NH ₂ + CH ₂ symmetric stretching
27	3,054	3,020		2,898	CH ₂ symmetric stretching
28	3,110	3,098	3,016		CH ₂ asymmetric stretching
29	3,281	3,266		3,170	NH ₂ symmetric stretching
30	3,349	3,340			NH ₂ asymmetric stretching

^a Scaling factor at the MP2/6-31+G(d) level of theory from Ref. [59]^b Experimental Raman data in aqueous solution from Ref. [26]^c Experimental IR data in aqueous solution from Ref. [27]

() was fully optimized by the ab initio QM/MM-FEG-NEB method with respect to glycine structural parameters at the HF/6-31+G(d) level, i.e., at the FE:HF/6-31+G(d)//FE:HF/6-31+G(d) level. On the other hand, the second one () was evaluated at the MP2/6-31+G(d) level along the FE reaction coordinate s optimized at the FE:HF/6-31+G(d) treatment, i.e., at the FE:MP2/6-31+G(d)//FE:HF/6-31+G(d) level. Then, in Fig. 6, the abbreviation FE:HF//FE:HF stands for the former profile, while FE:MP2//FE:HF does for the latter one. In comparison, the PE profiles are also drawn at both the

HF and MP2 level and are denoted similarly by PE:HF//FE:HF () and PE:MP2//FE:HF (), respectively.

In this study, we defined the FE reaction coordinate s (i.e., the reaction coordinate on FES) in a manner analogous to the intrinsic reaction coordinate (IRC) [62] as follows:

$$ds = \sqrt{\sum_j dr_j^2}, \quad (17a)$$

$$dr_j = (\sqrt{m_j}dx_j, \sqrt{m_j}dy_j, \sqrt{m_j}dz_j), \quad (17b)$$

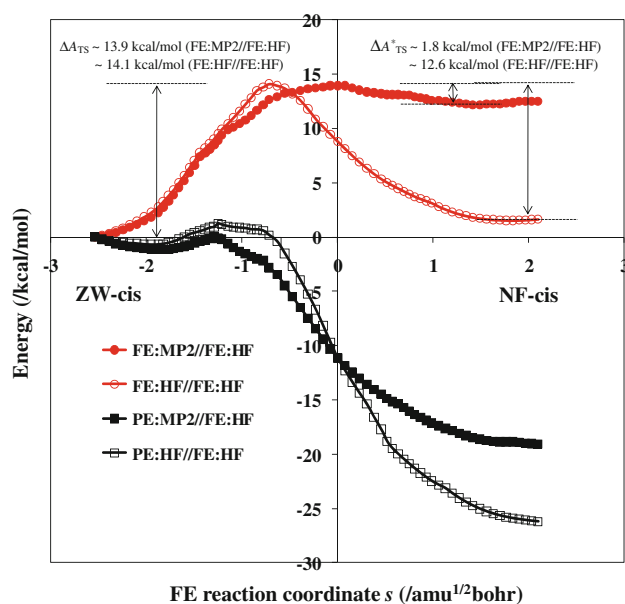


Fig. 6 Free energy (FE) profiles and potential energy (PE) ones for the intramolecular proton transfer process of the glycine molecule in aqueous solution at the HF/6-31+G(d) and the MP2/6-31+G(d) level of theory along the FE reaction coordinate s obtained by the FEG method at the FE:HF/6-31+G(d)//FE:HF/6-31+G(d) level

where m_j denotes the mass weight of the j th atom in the solute glycine molecule and (x_j, y_j, z_j) are its Cartesian coordinates. As a result, the FEs of activation from the reaction ZW-cis to NF-cis, ΔA_{TS} were estimated to be 13.9 kcal/mol at the FE:MP2//FE:HF level and 14.1 kcal/mol at the FE:HF//FE:HF level, respectively.

These values are both smaller in comparison with 16.85 kcal/mol which was previously evaluated after the TS structural optimization by the EVB-FEG method [12–14], taking the IRC in gas phase as the reaction coordinate. Then, by taking the entropic effect of the solute glycine molecule into consideration so as to compare the present ΔA_{TS} with those by the umbrella sampling method using CP-MD method [39], the free energetic contribution within the HA, δA_{TS}^{HA} , was obtained to be 0.1 kcal/mol at the FE:HF//FE:HF level, and the corrected ΔA_{TS} correspond reasonably to 12.7 kcal/mol, namely the estimation by the CP-MD method [39]. Finally, to compare them with the experimental one, we have estimated also the free energetic contribution of the ZPE, which was -3.3 kcal/mol at the FE:HF//FE:HF level and was neglected in the previous report by the CP-MD method [39]. By including both free energetic contributions through Eq. 16a, ΔA_{TS} were finally evaluated 10.7 kcal/mol at the FE:MP2//FE:HF level and 10.9 kcal/mol at the FE:HF//FE:HF level and were, however, underestimated than the experimental 14.4 kcal/mol [25]. This should be partly because (1) the

present TS structure was optimized at the HF/6-31+G(d) level and (2) we employed the general GAFF parameters [44] as a set of QM-MM LJ parameters at all positions along the reaction coordinate.

On the other hand, the FE of activation of the inverse reaction from NF-cis to ZW-cis, ΔA_{TS}^* , is 1.8 kcal/mol at the FE:MP2//FE:HF level and was in good agreement with the previous “theoretical” estimations, e.g., 0.65–2.5 kcal/mol by some quantum chemical calculations [34–36, 39]. However, ΔA_{TS}^* at the FE:HF//FE:HF level was overestimated in comparison with the above previous estimations, as well as that by EVB-FEG method [12, 13], where the EVB potential was originally calibrated on the basis of the PES calculation at the HF level. The FE overestimation, therefore, could be understood by the artifactual error of the PE at the HF level as shown in Fig. 6. Even if the ab initio QM/MM-FEG-NEB method was used, for discussion of the FE stability of the proton transfer reaction of glycine in aqueous solution, it would be essentially necessary to include the electron correlation effect in the ES calculation at least at the MP2 level.

4 Conclusion

For the purpose to explore the accurate reaction path for a chemical reaction system in solution, we have proposed the ab initio QM/MM-FEG method. For demonstration, the ab initio QM/MM-FEG method has been applied to the intramolecular proton transfer reaction from ZW-cis to NF-cis of glycine in aqueous solution.

First, we have obtained the optimized molecular structures of the solute glycine at ZW-cis and NF-cis on the FES in aqueous solution. Including the solvent effect explicitly, these structures were found to be different from those obtained in gas phase and by the CPCM method. Additionally, it was shown that the vibrational frequencies at the optimized structure of ZW-cis by the FEG method are compared reasonably well with the experimental Raman and IR frequencies of glycine in aqueous solution.

Next, according to the VFA in aqueous solution, we have obtained the TS structure on the FES which was shown to have only one imaginary frequency. As a result, the FE of activation of the reaction from ZW-cis to NF-cis was found in good agreement with the estimation by the CP-MD method, being underestimated in comparison with the experimental one. This should be attributed to the neglect of the electron correlation effect in the ES calculation for the TS optimization, and/or the inadequate QM-MM LJ parameters for the QM/MM-MD simulation. On the other hand, the FE of activation from NF-cis to ZW-cis was obtained as 1.8 kcal/mol at the FE:MP2//FE:HF level

and was in good agreement with the previous “theoretical” estimations, while that at the FE:HF//FE:HF level was overestimated. This overestimation of FE should be originating in the error of PE itself due to the lack of the electron correlation effect. One can understand, therefore, that for the discussion of the FE stability of the proton transfer reaction of glycine in aqueous solution, it is essentially necessary to include the electron correlation effect in the ES calculation.

In addition, it should be noticed that the present FEG method was based on the transition state theory [53] as well as most of DCMs and, therefore, does not include usually the non-adiabatic effect for the proton transfer reaction in solution. Even after we would improve the present FEG treatments so as to resolve the remaining problems such as the insufficient QM calculation level and the unsuitable QM–MM parameters, if the calculation results by the FEG method would not be able to represent the experimental ones, such incompleteness should be due to the neglect of the non-adiabatic effect.

The ab initio QM/MM–FEG method is computationally very expensive in comparison with some methodologies with the mean field approximation such as the DCMs. However, it should be the final goal of theoretical chemists that is to clarify the microscopic mechanism of the solution reaction systems on the FES exactly beyond the naïve treatments. In future, therefore, it is convinced that with the significant increase in computational resources, a number of applications of the ab initio QM/MM–FEG method must expand the scope of computational and theoretical methodologies toward the more complex solution reaction systems such as the enzyme-catalyzed ones in vivo. Such studies are in progress in our group [63].

Acknowledgments This work was supported by the a Grant-in-Aid for Science Research from the Ministry of Education, Culture, Sport, Science and Technology, and also by Core Research for Evolutional Science and Technology (CREST) “High Performance Computing for Multi-scale and Multi-physics Phenomena” from the Japan Science and Technology Agency (JST).

References

- Warshel A (1991) *Computer Modeling of Chemical Reactions in Enzymes and Solutions*. Wiley-Interscience, New York
- Gao J, Thompson MA (1998) *Combined Quantum Mechanical and Molecular Mechanical Methods*. American Chemical Society, Washington
- Santiso EE, Gubbins KE (2004) *Mol Simul* 30:699
- Vayner G, Houk KN, Jorgensen WL, Brauman JI (2004) *J Am Chem Soc* 126:9054
- Tomasi J, Mennucci B, Cammi R (2005) *Chem Rev* 105:2999
- Geerke DP, Thiel S, Thiel W, van Gunsteren WF (2007) *J Chem Theor Comput* 3:1499
- Sato M, Yamataka H, Komeiji Y, Mochizuki Y, Ishikawa T, Nakano T (2008) *J Am Chem Soc* 130:2396
- Chipot C, Pohorille A (2007) *Free energy calculations: theory and applications in chemistry and biology*. Springer, Berlin
- Okuyama-Yoshida N, Nagaoka M, Yamabe T (1998) *Int J Quantum Chem* 70:95
- Car R, Parrinello M (1985) *Phys Rev Lett* 55:2471
- Field MJ, Bash PA, Karplus M (1990) *J Comp Chem* 11:700
- Okuyama-Yoshida N, Nagaoka M, Yamabe T (1998) *J Phys Chem A* 102:285
- Nagaoka M, Okuyama-Yoshida N, Yamabe T (1998) *J Phys Chem A* 102:8202
- Okuyama-Yoshida N, Kataoka K, Nagaoka M, Yamabe T (2000) *J Chem Phys* 113:3519
- Warshel A, Weiss RM (1980) *J Am Chem Soc* 102:6218
- Hirao H, Nagae Y, Nagaoka M (2001) *Chem Phys Lett* 348:350
- Nagae Y, Oishi Y, Narse N, Nagaoka M (2003) *J Chem Phys* 119:7972
- Nagaoka M, Nagae Y, Koyano Y, Oishi Y (2006) *J Phys Chem A* 110:4555
- Takenaka N, Koyano Y, Nagaoka M (2010) *Chem Phys Lett* 485:119
- Takenaka N, Koyano Y, Nakagawa Y, Nagaoka M (2010) *J Comp Chem* 31:1287
- Koyano Y, Takenaka N, Nakagawa Y, Nagaoka M (2010) *Bull Chem Soc Jpn* 83:486
- Koyano Y, Takenaka N, Nakagawa Y, Nagaoka M (2010) *J Comp Chem* 31:2628
- Haberfield P (1980) *J Chem Educ* 57:346
- Wada G, Tamura E, Okina M, Nakamura M (1982) *Bull Chem Soc Jpn* 55:3064
- Slifkin MA, Ali SM (1984) *J Mol Liquids* 28:215
- Furić K, Mohaček V, Bonifačić M, Štefanić I (1982) *J Mol Struct* 267:39
- Kumar S, Rai AK, Singh VB, Rai SB (2005) *Spectrochim Acta Part A* 61:2741
- Császár AG (1992) *J Am Chem Soc* 114:9568
- Jensen JH, Gordon MS (1995) *J Am Chem Soc* 117:8159
- Kwon OY, Kim SY, No KT (1995) *Bull Korean Chem Soc* 16:410
- Selvarengan P, Kolandaivel P (2002) *THEOCHEM* 617:99
- Bachrach SM (2008) *J Phys Chem A* 112:3722
- Tortonda FR, Pascual-Ahuir JL, Silla E, Tuñón I (1996) *Chem Phys Lett* 260:21
- Tuñón I, Silla E, Ruiz-López MF (2000) *Chem Phys Lett* 321:433
- Kassab E, Langlet J, Evleth E, Akacem Y (2000) *THEOCHEM* 531:267
- Bandyopadhyay P, Gordon MS, Mennucci M, Tomasi J (2002) *J Chem Phys* 116:5023
- Yamabe S, Ono N, Tsuchida N (2003) *J Phys Chem A* 107:7915
- Balta B, Aviyente V (2003) *J Comp Chem* 24:1789
- Leung K, Rempe SB (2005) *J Chem Phys* 122:184506
- Takahashi H, Kawashima Y, Nitta T (2005) *J Chem Phys* 123:124504
- Lu Z, Zhang Y (2008) *J Chem Theor Comput* 4:1237
- Yoshikawa T, Motegi H, Kakizaki A, Takayanagi T, Shiga M, Tachikawa M (2009) *Chem Phys* 365:60
- Jorgensen WL, Chandrasekhar J, Madura JD (1983) *J Chem Phys* 79:926
- Wang J, Wolf RM, Caldwell JW, Kollman PA, Case DA (2004) *J Comp Chem* 25:1157
- Okamoto T, Yamada K, Koyano Y, Asada T, Koga N, Nagaoka M (in press) *J Comp Chem* (doi:10.1002/jcc.21678)
- Cheng A et al (2002) ROAR 2.1. The Pennsylvania State University
- Case DA et al (2002) AMBER 7. University of California, San Francisco

48. Frisch MJ et al (2004) Gaussian03, revision C. 02. Gaussian Inc, Wallingford
49. Zwanzig RW (1954) *J Chem Phys* 22:1420
50. Liu DC, Nocedal J (1989) *Math Prog* 45:503
51. Jónsson H, Mills G, Jacobsen KW (1998) *Classical and quantum dynamics in condensed phase simulations*. World Scientific, Singapore, p 385
52. Galván IF, Sánchez ML, Martín ME, Olivares del Valle FJ, Aguilar MA (2003) *J Chem Phys* 118:255
53. Glasstone S, Laidler KJ, Eyring H (1941) *The theory of rate processes*. McGraw-Hill, New York
54. McQuarrie DA (1976) *Statistical mechanics*. Harper and Row, New York
55. Nagaoka M, Okamoto T, Maruyama Y (2002) *J Chem Phys* 117:5594
56. Singh UC, Kallman PA (1984) *J Comp Chem* 5:129
57. Besler BH, Merz KM Jr, Kallman PA (1990) *J Comp Chem* 11:431
58. Barone V, Cossi M (1998) *J Phys Chem A* 102:1995
59. Merrick JP, Moran D, Radom L (2007) *J Phys Chem A* 111:11683
60. Schmitt UW, Voth GA (1999) *J Chem Phys* 111:9361
61. Wu Y, Tepper HL, Voth GA (2006) *J Chem Phys* 124:024503
62. Fukui K (1970) *J Phys Chem* 74:461
63. Asada T, Takenaka N, Koyano Y, Yamada K, Okamoto T, Nagaoka M (2011) *J Phys Chem B*, to be submitted